

Geochemical Characteristics of Precambrian, Jurassic and Cretaceous Granites in Korea

Young Kook Hong*

Abstract: The geochemical characteristics including minerals, major and trace elements chemistries of the Proterozoic, Jurassic and Cretaceous granites in Korea are systematically summarized and intended to decipher the origin and crystallization process in connection with the tectonic evolution.

The granites in Korea are classified into three different ages of the granites with their own distinctive geochemical patterns: 1) Proterozoic granitoids; 2) Jurassic granites (cratonic and mobile belt); 3) Cretaceous—Tertiary granites.

The Proterozoic granite gneisses (I-type and ilmenite-series) formed by metamorphism of the geochemically evolved granite protolith. The Proterozoic granites (S-type and ilmenite-series) produced by remobilization of sialic crust. The Jurassic granites (S-type and ilmenite-series) were mainly formed by partial melting of crustal materials, possibly metasedimentary rocks. The Cretaceous granites (I-type and magnetite-series) formed by fractional crystallization of parental magmas from the igneous protolith in the lower crust or upper mantle.

The low temperature (315~430°C) and small temperature variations ($\pm 20\sim 30^\circ\text{C}$) in the cessation of exsolution of perthites for the Proterozoic and Jurassic granites might have been caused by slow cooling of the granites under regional metamorphic regime. The high (520°C) and large temperature variations ($\pm 110^\circ\text{C}$) of perthites for the Cretaceous granites postulate that the rapid cooling of the granitic magma.

In terms of the oxygen fugacity during the feldspar crystallization in the granite magmas, the Jurassic mobile belt granites were crystallized in the lowest oxygen fugacity condition among the Korean granites, whereas the Cretaceous granites in the Gyeongsang basin at the high oxygen fugacity condition.

The Jurassic mobile belt granites are located at the Ogcheon Fold Belt, resulting by closing-collision situation such as compressional tectonic setting, and emplaced into a Kata-Mesozonal ductile crust. The Jurassic cratonic granites might be more evolved either during intrusion through thick crust or owing to lower degree of partial melting in comparison with the mobile belt granites. The Cretaceous granites are possibly comparable with a continental margin of Andinotype. Subduction of the Kula-Pacific ridge provided sufficient heat and water to trigger remelting at various subcrustal and lower crustal igneous protoliths.

INTRODUCTION

Among the plutonic rocks, granitoids are most predominant, covering approximately 30% of the whole surface of the Republic of Korea (hereafter

called the Korea). The Korean peninsula has history of prolonged and varied plutonism, lasting from early middle Precambrian (2,154—1,530 Ma) through Jurassic (205—153 Ma) to Cretaceous—Tertiary (120—41 Ma) time (Fig. 1).

Three temporal variations of granite in Korea have been delineated each with its own distin-

* Korea Institute of Energy and Resources
219-5, Garibong-dong, Guro-gu, Seoul.

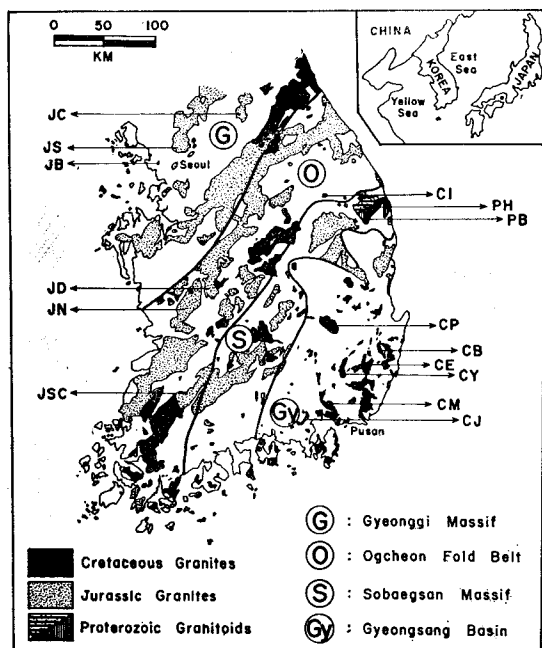


Fig. 1 Map of the Republic of Korea showing the distribution of granitic rocks and studied granites for this work. The map is generally based on the Geological map of Korea (KIER, 1981). PB: Proterozoic Buncheon granite gneiss, PH: Proterozoic Hongjesa granite, JS: Jurassic Seoul granite, JB: Jurassic Bupyeong granite, JC: Jurassic Chuncheon granite, JD: Jurassic Daejeon granite, JN: Jurassic Nonsan granite, JSC: Jurassic Sunchang granite, CI: Cretaceous Imog granite, CM: Cretaceous Masan granite, CJ: Cretaceous Jindong granite, CB: Cretaceous Bulgugsa granite, CP: Cretaceous Palgongsan granite, CE: Cretaceous Eonyang granite, and CY: Cretaceous Yoocheon granite.

ctive petrochemical pattern: the Proterozoic granitoids; the Jurassic granites (cratonic and mobile belt); the Cretaceous—Tertiary granites.

1. The Proterozoic granitoids: Major batholiths of I-type granite gneiss and S-type granite are present, all of ilmenite-series.

2. The Jurassic granites: The granites can be further divided into cratonic and mobile belt granites. The large batholiths are S-type and ilmenite-series, and compositionally restricted.

3. The Cretaceous—Tertiary granites: Oval and irregular stocks of compositionally expanded,

suite of I-type and magnetite-series.

The purposes of this study are to summarize systematically the contrasting geochemical characteristics of Proterozoic, Jurassic, and Cretaceous granites in Korea and to present a unified body of petrochemical data in connection with the tectonic evolution. Fifteen representative granite bodies are geochemically studied in this work (Fig. 1).

GENERAL CHARACTERISTICS OF THE GRANITES

The general contrasting field occurrence and petrological characteristics of the Proterozoic, Jurassic and Cretaceous—Tertiary granites form the basis for a subdivision of the granitic rocks in Korea (Table 1).

The Proterozoic Granitoids

The granitoids consisting of granite gneisses (Buncheon and Pyeonghae) and granites (Hongjesa, Naedeog and Nonggeori) are principally concentrated in the northeastern part of the Sobaegsan massif (Fig. 1). The medium to coarse grained granite gneisses (Buncheon and Pyeonghae) display gneissose structure, and intruded into the Precambrian metasedimentary rocks. The radiometric age determination on the granite gneisses show 2,107~2,154Ma (about 2.1Ga) by Rb/Sr whole-rock method with the initial $^{87}\text{Sr}/^{86}\text{Sr}$ ratios of 0.7082~0.7056 and 0.7079 (Hong, 1985b; Choo and Kim, 1985). The granite gneisses consist of quartz, microcline, oligoclase, biotite, zircon and apatite. Quartz crystals occur generally as large grains with undulose extinctions. Microcline presents typical gridiron twinning combined with albite and pericline twins. Plagioclase is identified as oligoclase (An 14~20) forming albite twinning and partly altered to sericite. Poikilitic biotite with inclusions of zircon and apatite lie parallel to elongated quartz and feldspar grains displaying augen porphyroblastic textures. In distinctly

Table 1 General summary of the characteristics of granites in Korea(modified from Jin, 1986).

	Proterozoic	Jurassic	Cretaceous-Tertiary
Shape	Sub-circular(batholith)	Long band(batholith)	Oval and irregular(stock)
Emplacement	Meso or Katazone	Meso or Katazone	Epizone
Structure & Occurrence	Granodiorite-Granite with little volcanic association With foliation Horizontal joints are common Pegmatites are abundant Schlieren and xenolith or skialiths of gneiss and schist are abundant	Quartz diorite-Granodiorite-Granite with little volcanic association(migmatite) With foliation Horizontal joints are common Pegmatitic or QTZ veins are abundant Basic segregation, schlieren, and xenoliths or skialiths of gneiss and schist are abundant	Tonalite-Granodiorite-Granite with abundant volcanic association such as andesite-dacite-rhyolite Without any foliation Vertical joints are common Aplitic or QTZ veins are abundant Xenoliths of volcanic rocks of sedimentary rocks are abundant
Contacts	Concordant	Concordant	Sharp(hornfels)
Cooling history	Slow cooling	Slow cooling	Rapid cooling
Texture	Medium to coarse grained QTZ grains can be easily observed with naked eyes (euhedral or subhedral) Graphic textures are hardly seen Porphyroblastic	Medium to coarse grained QTZ grains can be easily observed with naked eyes (euhedral or subhedral) Graphic textures are scarcely seen Porphyroblastic and porphyroclastic	Fine to medium grained QTZ grains can be hardly observed with naked eyes(interstitial) Graphic and miarolitic textures are seen Porphyritic
Mineral composition	K-feldspar is mainly microcline Some QTZ show undulatory extinction Two-mica or Muscovite-free With tourmaline, garnet and myrmekite	K-feldspar is mainly microcline or perthite QTZ shows undulatory extinction Two-mica With garnet and myrmekite	K-feldspar is mainly microperthite or orthoclase QTZ shows little undulatory extinction Muscovite-free With tourmaline and sulfide minerals (myrmekite rare)
Mineralization	None	CaF ₂ , Au, Ag mineralization	Cu, Pb, Zn, Mo and W mineralization
Magnetic susceptibility	30×10^{-6} emu/g, n=74 (ilmenite-series)	48×10^{-6} emu/g, n=132 (ilmenite-series)	306×10^{-6} emu/g, n=247 (magnetite-series)
Sr initial ratios	0.7056~0.7229	0.7107~0.7176	0.7040~0.7070

foliated granite gneisses, the foliation is caused by bands and streaks of recrystallized feldspar and quartz, and by an increased amount of biotite in streaky aggregates. With geochemical evidences and magnetic susceptibility measurements (about 30×10^{-6} emu/g), the granite gneisses are reported to be formed by metamorphism from the geochemically evolved igneous protolith such as I-type granitic rocks in which plagioclases were already depleted, and belong to the ilmenite-series(Hong, 1985b).

The Proterozoic granites (Hongjesa, Naedeog and Nonggeori) are generally characterized by dark grey and blue coloured medium to coarse grained alkali-feldspar, light coloured plagioclase, quartz, biotite, muscovite, tourmaline, garnet, zircon, apatite and opaques. Subhedral and mostly fractured quartz grains have strong undulose extinctions and are interlocked with each other. Myrmekitic intergrowth around quartz and feldspar is observed in some places. Microcline is predominant with cross-hatched

twinning. Plagioclase occurs as subhedral oligoclase (An 16~28) with parallel twinning. Rb/Sr whole-rock isochrons for the Hongjesa granite (PH) have been measured as ages of 1.71 Ga with an initial $^{87}\text{Sr}/^{86}\text{Sr}$ ratios of 0.7229 (Kim et al., 1978) and of 1.75 Ga with 0.7174 (Choo and Lee, 1980). The K-Ar ages on muscovite of the Nonggeori granite show 1,530Ma (Ueda, 1969), 1,762Ma (Farrar et al., 1978) and 1,736-1,802Ma (Yun, 1983). Radiometric age determination on the Naedeog granite reveals as 1,642-1,787Ma by K-Ar dating on muscovite (Yun, *op cit*). The granites are known to be produced by remobilization of sialic crust (S-type) and belong to the ilmenite-series (Hong, 1985b; Yun, 1985). Anatexis was probably the main function for producing the Proterozoic granites in NE part of the Sobaegsan massif.

The Jurassic Granites

The Jurassic occur widely as batholiths with NE-SW elongation (Sinian direction) and a width of 30-50Km. The Jurassic granites can further divided into cratonic (Gyeonggi massif) and mobile belt (Ogcheon Fold Belt) granites (Fig. 1); The former shows somewhat sharp contact relations, whereas the latter is structurally rather concordant with the Precambrian metasedimentary rocks. No contact metamorphic aureoles such as chilled margins are observed in the country rocks which are adjacent to the granites. Volcanic rocks and pegmatite have not been recognized often in the surrounding areas around the granites. This is possibly the result of uplift and erosion in late Jurassic Daebo orogeny which resulted in the removal of the upper part of the batholiths, together with their volcanic products. But, schlieren and xenolith of metasedimentary rocks, and basic segregation are abundant in the Jurassic granites, predominantly in the Ogcheon Fold Belt. The granites are mostly medium to coarse grained (3-5mm) and do not vary significantly in grain

size (equigranular to porphyroblastic textures), and range from quartz diorite through granodiorite to quartz monzonite (adamellite), granodiorite being the most abundant. Most of the quartz grains in the Jurassic granites can be easily identified individually with the naked eye owing to coarse size and sub to euhedral shape of the grains. The measurement of magnetic susceptibility on the Jurassic granites an average of 48×10^{-6} emu/g and belong to the ilmenite-series.

The Jurassic cratonic granites in the Gyeonggi massif are largely homogeneous in texture and mineral composition. The granites are usually coarse-grained with a slight reddish potash feldspar, milky white plagioclase, light-grey subrounded equigranular quartz, biotite, muscovite, zircon and apatite. The cratonic granites are dated by Rb/Sr whole-rock method giving ages of 160-205Ma with initial $^{87}\text{Sr}/^{86}\text{Sr}$ values of 0.712-0.715 (Park, 1972; Jin et al., 1986).

The Jurassic mobile belt granites in the Ogcheon Fold Belt are syntectonic subsolvus granites, mainly consisting of microcline, oligoclase, quartz, biotite and muscovite. The mobile belt granites show considerable variation in texture and mineral components. The granites are generally medium to coarse grained and ubiquitously display foliated textures. The granites have been radiometrically dated as 153-190Ma with initial $^{87}\text{Sr}/^{86}\text{Sr}$ ratios of 0.711-0.718 by Rb/Sr whole rock method (Choo et al., 1982).

Ore mineralization associated with the S-type Jurassic granites is very rare except some CaF_2 , Au and Ag mineralization related with quartz veins.

The Cretaceous-Tertiary Granites

The Cretaceous-Tertiary granites occur as batholiths, small scattered oval, and irregular plutons generally in the Gyeongsang basin (Fig. 1). The granites are surrounded by narrow

contact metamorphic zones of hornfels up to 2km wide and some have miarolitic cavities, which is considered to imply epicrustal emplacement and to denote the presence of abundant volatile components in the magma. The contacts between the plutons and the sedimentary country rocks are sharp, tectonically disturbed and steeply dipping outward radially (Jin, 1980; 1982). The contact zones show a large number of xenoliths of sedimentary and volcanic rocks which have been almost digested by the granites. Particularly, needle-like hornblende bearing xenoliths derived from volcanic rocks have been commonly observed. The granites intruded at a shallow crustal level into the sedimentary and volcanic rocks along the weak zones in NNE-NE direction apparently along the ring faults derived from the cauldron subsidence. The granites show conspicuous zonations and are almost porphyritic in texture, or occasionally uneven in grain size, ranging from fine to medium, inward from the margin. Quartz in the granites is interstitial, fills the boundaries between the feldspars and shows micrographic texture. The Cretaceous-Tertiary granites are characterized by the presence of microperthite, orthoclase, and hornblende, whilst microcline and biotite are greatly abundant in the Jurassic granites; the latter may have crystallized slowly at a low temperature. The $^{87}\text{Sr}/^{86}\text{Sr}$ initial ratios for the granites (120-41Ma) range from 0.704 to 0.707 (Jin, 1980) which denotes that the granites were essentially derived from igneous protolith. The granites are mainly of I-type and magnetite-series (mean of 306×10^{-6} emu/g), and quartz diorite through granodiorite to quartz monzonite and granite range from in composition with quartz monzonite predominating.

The average chemical composition of the Cretaceous-Tertiary granitic rocks is more silicic compared with the composition of the

Jurassic granitoids. Polymetallic mineralization in the form of small vein and breccia pipe deposits containing variable proportions of Cu, Pb, Zn, Au, Mo, W, Ag and As minerals exclusively associated with relatively intensive wall-rock alteration most commonly in the Cretaceous-Tertiary granites (Jin, et al., 1981). This metallogenetic pattern was generated by cal-alkaline magmatism which, by analogy with central Andean metallogeny, occurred above a shallow, northward-dipping subduction zone (Sillitoe, 1977).

MINERAL CHEMISTRY OF THE GRANITES

Analyses of the rock-forming minerals such as alkali-feldspar, plagioclase and biotite were made on the Korean granites with an energy dispersive electron microprobe. Study for the mineral chemistry is confined on the granites ranging from 66% to 75% of SiO_2 content (*Sensu stricto*). The main purpose of mineral analyses for the 37 representative granites is to elucidate chemical variations in each mineral phase through magmatic evolution. The conditions of analysis, calibration and correction procedures were as described by Sweatman and Long (1969), Statham (1976), and Hong (1983a).

Chemistry of Alkali-Feldspar

The alkali-feldspars in the studied Korean granites show microperthitic to perthitic textures. The analytical results given in Table 2 are microprobe analyses of exsolved grains. The number of cation Na in the alkali-feldspar is higher in the Cretaceous granites (0.25) than in the Proterozoic and Jurassic granites (0.04-0.08). In contrast, the numbers of cation K in the alkali-feldspar is higher in the Proterozoic and Jurassic granites (0.89-0.97) than in the Cretaceous granites (0.71). The numbers of cation Ca in the exsolved plagioclase is higher in the Jurassic mobile belt and Cretaceous

Table 2 Average number of cations and temperatures of cessation of exsolution in perthites for the granites in Korea.

Numbers in parentheses show the numbers of samples analysed.

	Proterozoic Granite PH (4)		Jurassic Granite				Cretaceous Granite (CP, CE, CY; 16)	
	AF	PL	Cratonic (JS; 8)		Mobile belt (JD, JN; 9)		AF	PL
			AF	PL	AF	PL		
Si	2.99±0.01	2.95±0.04	3.05±0.01	2.97±0.03	2.99±0.01	2.71±0.03	3.00±0.02	2.87±0.06
Al	1.00±0.01	1.05±0.04	1.00±0.01	1.03±0.03	1.02±0.02	1.29±0.03	1.00±0.02	1.12±0.05
Fe	0.02±0.01	—	—	—	—	—	0.06	—
Ca	0.01±0.01	0.06±0.04	—	0.03±0.03	—	0.30±0.03	—	0.13±0.06
Ba	—	—	—	—	0.01	—	0.01±0.01	—
Na	0.04±0.01	0.95±0.03	0.05±0.01	0.95±0.02	0.08±0.01	0.69±0.03	0.24±0.12	0.85±0.07
K	0.97±0.01	0.01	0.93±0.01	0.02±0.01	0.89±0.01	0.01	0.71±0.13	0.02±0.01
T°C in 3Kb	330±21°C		315±18°C		410±26°C		519±107°C	
T°C in 5Kb	347±21°C		332±18°C		428±27°C		541±110°C	

$$T(K) = \frac{-X^2K(AF)[6330 + 0.093P + 2X_{Na}(AF)(1340 + 0.019P)]}{R \ln KD + X^2K(AF)[-4.63 + 1.54X_{Na}(AF)]}$$

$$R = 1.9872 \text{ cal, } KD = \frac{X_{Na}(AF)}{X_{Na}(PL)} \quad (\text{after Powell \& Powell, 1977})$$

granites (0.13–0.30) than in the Proterozoic and Jurassic cratonic granites (0.03–0.06). The numbers of cation Na in the exsolved plagioclase is a little higher in the Proterozoic and Jurassic cratonic granites (0.95) than in the Jurassic mobile belt and Cretaceous granites (0.69~0.85).

Alkali-feldspars in granitic rocks tends to exsolve into K-rich and Na-rich phases. Unmixing may have been complete, producing separate grains of optically homogeneous albite and K-feldspar, or the separation may have halted when the temperature dropped below that at which Na and K ions had sufficient thermal energy to migrate through the feldspar structure (Brown and Parson, 1981). In complete exsolution yield lamellae or patches of one phase within the other such as perthite. Determination of geological temperature based on the distribution of albite (Na) component between two coexisting feldspars (perthite) is of great practical significance. Barth (1962) proposed a semi-

empirical two-feldspar geothermometer, based on the distribution of $NaAlSi_3O_8$ between coexisting plagioclase and alkali-feldspar from natural assemblages. More recent workers (Bath, 1968; Stormer, 1975; Powell and Powell, 1977; Ferry, 1978) have attempted to improve in Barth's formulation by using a temperature calibration based on experimental determinations of feldspar solvus relations or exchange reactions.

The numbers of cation K and Na of the perthitic alkali-feldspars in Proterozoic granites illustrate a small variance (Table 2). Using Powell and Powell's geothermometer equation (1977), calculated temperatures for cessation of exsolution show a narrow range of about $330 \pm 20^\circ\text{C}$ at an assumed pressure of $>3\text{Kbar}$ from normative Q-Ab-Or ternary diagram (Hong, 1985b).

The numbers of cations K and Na in the Jurassic perthitic alkali-feldspars do not show any significant trend (Table 2). The graphical representation of geothermometer by Stormer

(1975) illustrates that the Jurassic perthites plot in small range which shows little temperature variation in each granite body. The calculated temperatures for cessation of exsolution in the perthitic alkali-feldspars remain within a generally narrow range of about 40°~60°C difference in each granite as a spatial whole. The cessation temperature of perthite exsolution in the Jurassic mobile belt granites is higher than in the Jurassic cratonic granites, 430°C and 330°C at an assumed pressure of 5 Kbar from normative Q-Ab-Or diagram (Hong, 1984a; 1984b) respectively. The small temperature variation of the perthites in Jurassic granites could be explained as the country rocks adjacent to the granites had been under regional metamorphic regime (Daeboro orogeny) during the intrusion and those rocks had cooled down slowly.

The average temperature of cessation of exsolution in the Cretaceous perthitic alkali-feldspars is about 520°C at an assumed pressure of >3Kbar (Hong, 1983b; 1985a). The number of cations K and Na in the Cretaceous granites shows a large variation, and the temperatures of exsolution generally decrease from margin to central part in each granite stock with about 220°C differences. The cation Na in the alkali-feldspar is much higher relative to the Jurassic granites. The large differences in temperatures of cessation of exsolution in Cretaceous perthites postulate that the rapid cooling of the granitic magma provoked the formation of a kind of solidified shell in the outer part of the intruded mass. The heat flow of the country rocks in contact with the intruding Cretaceous granites is assumed to be small. The shell was rather impermeable and hence the differences in temperature of cessation of perthite exsolution should be large.

Chemistry of Plagioclase

Plagioclase analytical results are presented in Table 3. Numbers of cation Ca in plagioclase

Table 3 Electron microprobe analyses of plagioclase in the granites.

	Proterozoic Granite (PH; 4)	Jurassic Granite		Cretaceous Granite (CP, CE, CY; 7)
		Cratonic (JS; 7)	Mobile belt (JN, JD; 7)	
SiO ₂	66.3±0.7	66.3±0.7	60.8±1.2	64.7±1.3
Al ₂ O ₃	20.8±0.6	20.8±0.7	25.0±0.9	21.9±0.9
FeO(t)	—	—	—	0.12±0.08
CaO	1.8±0.6	1.9±0.5	6.4±0.9	3.0±1.00
Na ₂ O	10.7±0.3	10.6±0.4	8.0±0.5	9.8±0.7
K ₂ O	0.1	0.3±0.2	0.1±0.1	0.4±0.1
Recalculated on 8 Oxygens				
Si	2.92±0.03	2.92±0.03	2.69±0.04	2.85±0.05
Al	1.08±0.03	1.08±0.03	1.31±0.05	1.14±0.05
Fe	—	—	—	—
Ca	0.08±0.03	0.09±0.03	0.30±0.04	0.15±0.05
Na	0.91±0.03	0.90±0.03	0.69±0.04	0.84±0.06
K	0.01	0.02±0.01	0.01	0.02±0.01
Mole Proportion (%)				
Or	0.8±0.2	1.7±1.1	0.8±0.4	2.2±0.8
Ab	90.8±3.1	89.5±2.6	68.7±4.0	83.6±5.3
An	8.5±3.0	8.8±2.6	30.5±4.3	14.2±4.8

are 0.30 in the Jurassic mobile belt, 0.15 in the Cretaceous, and 0.08~0.09 in the Proterozoic and Jurassic cratonic granites. The chemistry of plagioclase reflects that the Proterozoic and Jurassic granites (high alkali cations and low cation Ca) are more evolved than the Jurassic mobile belt and Cretaceous granites. Mole proportion of An is higher in the Jurassic mobile belt granite as calcic as An₃₀ compared with the other Korean granites (An_{9~14}).

Chemistry of Biotite

The major element concentrations of biotites are analysed on the Mesozoic granites and their structural formulae are given in Table 4. The numbers of cation Fe and Al of biotites in the Jurassic granites are higher than in the Cretaceous granites. But, the numbers of cation Mg and Ti are higher in the Cretaceous granites relative to the Jurassic granites. Ionic Fe/(Fe+Mg) ratio is generally higher in the Jurassic

Table 4 Microprobe analyses of biotites in the Mesozoic granites.

	Jurassic Granite		Cretaceous Granite (CP, CE, CY; 20)
	Cratonic (JS; 7)	Mobile belt (JD, JN; 7)	
SiO ₂	36.8± 0.7	35.8± 0.7	38.5± 0.9
Al ₂ O ₃	14.5± 0.6	15.8± 1.0	12.7± 0.5
TiO ₂	3.0± 0.5	2.5± 0.5	3.8± 0.8
FeO(t)	21.3± 1.5	21.8± 1.5	17.0± 2.6
MgO	8.2± 1.8	8.7± 1.7	13.6± 1.9
MnO	1.4± 0.6	0.4± 0.2	0.5± 0.3
CaO	—	0.1	—
K ₂ O	9.4± 0.2	9.5± 0.3	9.4± 0.3

Recalculated on 11 Oxygens

Si	2.87±0.03	2.80±0.04	2.90±0.05
Al	1.34±0.06	1.46±0.09	1.13±0.04
Ti	0.17±0.03	0.15±0.03	0.21±0.05
Fe	1.39±0.12	1.42± 0.1	1.07± 0.2
Mg	0.95±0.20	1.01± 0.2	1.51± 0.2
Mn	0.09±0.04	0.03±0.01	0.03±0.02
Ca	—	0.01	—
K	0.94±0.02	0.94±0.03	0.91±0.02
Fe/(Fe+Mg)	0.60±0.07	0.72±0.05	0.42±0.08

granites (0.60~0.72) than in the Cretaceous granites (0.42); which is possibly because more Fe has been consumed to form Fe-Ti oxide minerals in the latter granite.

WHOLE-ROCK CHEMISTRY OF THE GRANITES

Discussion on the geochemical characteristics of the granites in Korea is based upon the results of analyses on 156 granitoids for major and trace elements, and 74 granites in the narrow sense (*Sensu stricto*) for rare earth elements. Study for the primordial mantle-normalized trace element patterns (Figs. 3, 5, 7 and 9) are confined on the granites ranging from 66% to 75% of SiO₂ content (*Sensu stricto*). The analytical results are given in Tables 5, 6, and 7. The localities of the studied granite regions are shown in Fig. 1. Bulk rock major

and trace elements were analysed by XRF spectrometry on fused glass discs and pressed powder pellets, respectively. The concentrations of the rare earth elements were determined by instrumental neutron activation analysis (INAA). Detailed accounts and reviews on the geochemistry of each granite region have been presented by Hong (1983a, b; 1984a, b; 1985a, b; 1986), Tsusue et al (1984) and Seo (1985).

The Proterozoic Granitoids

The Proterozoic granitoids consist of granite gneiss and granite in the NE part of the Ogcheon Fold Belt (Fig. 1).

The Proterozoic granite gneiss (PB) shows: (1) A small variations in major element and high contents in SiO₂ from 72.32% to 76.83% with an average of 74.18±1.27%; (2) The normative corundum and molecular Al₂O₃/(Na₂O+K₂O+CaO) ratio are 1.27±0.4% and 1.02 respectively (3) A narrow range of variations with alkali-rich phase in the AFM diagram (Fig. 2); (4) The K₂O/Na₂O ratio of the granite gneiss is invariable from 1.23 to 1.57 with a mean of 1.43; (5) Clusters near the eutectic minimum signifying relatively low temperature

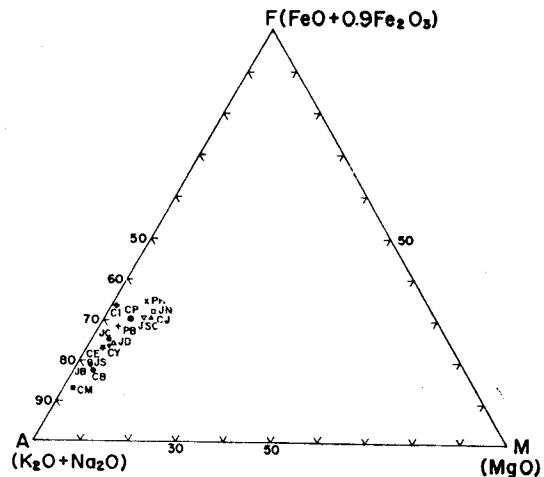


Fig. 2 AFM variation diagram of granites in Korea. symbols are as in Fig. 1.

Table 5 The average contents of major element of granites in Korea (in wt. %).
Numbers in parentheses show the numbers of samples analysed.
Data of JB after Seo (1985), and CM, CJ and CB after Tsusue et al (1984).

	Proterozoic		Jurassic						Cretaceous						
	PB (10)	PH (14)	Cratonic			Mobile Belt			CI (8)	CM (8)	CJ (4)	CB (14)	CP (16)	CE (21)	CY (9)
			JS (14)	JB (4)	JC (7)	JD (9)	JN (9)	JSC (9)							
SiO ₂	74.18	71.69	74.77	73.98	72.13	71.02	67.05	66.21	67.33	73.30	67.53	72.27	70.36	73.68	72.36
TiO ₂	0.19	0.32	0.16	0.18	0.23	0.27	0.60	0.45	0.20	0.18	0.39	0.26	0.34	0.23	0.28
Al ₂ O ₃	13.12	13.82	13.42	13.56	14.76	15.54	16.25	17.27	16.13	13.85	15.17	13.84	14.42	13.35	14.07
Fe ₂ O ₃	1.13	1.57	0.88	2.04	0.96	1.21	1.36	1.01	1.13	0.99	1.74	1.17	1.75	1.24	1.19
FeO	2.15	2.79	1.35	0.18	1.92	1.42	2.84	2.54	2.74	0.42	2.17	0.85	2.27	1.64	1.72
MnO	0.04	0.05	0.07	0.04	0.06	0.05	0.05	0.05	1.27	0.06	0.09	0.07	0.10	0.07	0.06
MgO	0.40	0.90	0.24	0.36	0.39	0.51	1.17	0.94	0.08	0.15	0.16	0.47	0.71	0.31	0.43
CaO	1.18	1.31	0.90	1.34	1.84	2.52	3.13	3.67	3.04	0.64	3.73	1.36	1.85	0.89	1.29
Na ₂ O	3.09	2.85	3.92	3.69	3.72	3.52	3.95	3.80	4.02	4.47	4.27	4.28	3.94	4.08	4.21
K ₂ O	4.40	4.23	4.51	4.49	4.12	3.76	3.48	3.12	3.36	4.01	2.86	4.28	4.10	4.40	4.32
P ₂ O ₅	0.05	0.12	0.04	0.07	0.08	0.10	0.18	0.03	0.09	0.04	0.09	0.07	0.11	0.06	0.07
Total	99.91	99.65	100.26	99.93	100.21	99.90	100.07	99.18	99.37	98.01	99.01	99.12	99.95	99.88	100.02
D.I	87.30	82.67	91.65	90.05	85.20	81.68	75.37	72.83	75.14	91.41	77.49	90.44	83.56	90.60	88.50
Norm. Corundum	1.27	2.45	0.57	0.76	1.35	1.33	0.70	1.16	0.94	—	—	0.20	0.42	0.40	0.39

Table 6 The average contents of trace element of granites in Korea (in ppm).
Numbers in parentheses show the numbers of samples analysed. Data of JB after Seo (1985), and CM, CJ and CB after Tsusue et al (1984). —: The element is not determined.

	Proterozoic		Jurassic						Cretaceous						
	PB (10)	PH (14)	Cratonic			Mobile Belt			CI (8)	CM (8)	CJ (4)	CB (14)	CP (16)	CE (21)	CY (9)
			JS (14)	JB (4)	JC (7)	JD (9)	JN (9)	JSC (9)							
Rb	296	210	209	193	123	142	126	116	135	114	86	130	134	151	136
Ba	267	655	509	—	784	756	1,038	544	716	557	393	583	742	620	738
Th	31	19	25	—	18	12	18	25	24	14	10	15	15	17	17
U	9.0	5.0	6.0	—	—	4.0	4.0	5.0	5.0	2.0	2.3	3.5	3.5	2.9	2.3
Li	53	60	59	—	24	42	41	—	46	—	—	—	47	33	51
Ta	1.54	1.15	1.40	—	—	1.15	0.34	1.66	0.94	0.99	0.60	1.29	1.37	1.11	1.30
Nb	13	13	19	12	26	21	11	14	10	9	8	10	13	13	13
Sc	6	8	4	—	4	2	3	—	8	—	—	—	5	4	6
Sr	72	178	147	—	234	487	643	472	109	54	270	134	222	114	158
V	20	34	16	8	20	17	46	35	67	—	—	—	42	19	23
Zn	36	58	43	20	50	65	77	41	50	—	—	—	62	37	53
Hf	2.92	7.65	4.13	—	—	5.73	5.54	4.57	4.07	4.42	2.40	3.96	4.39	4.71	8.97
Zr	123	148	93	46	70	165	194	267	193	—	—	—	185	155	196
Co	14	17	3	2	7	2	9	8	13	—	—	—	17	15	7
Cu	15	21	13	7	22	12	23	9	18	—	—	—	22	18	15
Y	47	20	23	—	17	17	9	25	23	—	—	—	24	30	34
K/Rb	123	167	179	193	278	220	229	223	247	292	275	274	254	242	264
Rb/Sr	4.1	1.2	1.4	—	0.5	0.3	0.2	0.2	1.2	2.1	0.3	1.0	0.6	1.3	0.9

Table 7 Rare earth elements analyses of the granites in Korea (in ppm).

	Proterozoic		Jurassic						Cretaceous						
			Cratonic			Mobile Belt									
	PB (3)	PH (4)	JS (4)	JB ⁺ (4)	JC ⁺ (6)	JD (2)	JN (4)	JSC (4)	CI (4)	CM (9)	CJ (4)	CB (14)	CP (5)	CE (5)	CY (2)
La	47.34	44.66	30.15	37.99	38.36	85.28	57.54	36.25	39.93	35.22	22.50	29.00	37.53	35.03	39.37
Ce	95.72	95.00	60.89	66.16	72.75	166.74	109.84	66.25	79.61	67.00	35.00	48.86	73.10	70.07	77.87
Nd	41.71	41.06	22.88	24.90	24.73	51.13	38.42	29.88	29.92	31.44	18.50	25.29	25.90	25.30	27.60
Sm	7.48	7.10	4.42	4.45	4.64	7.15	5.22	4.70	4.95	—	—	—	4.30	3.69	3.13
Eu	0.40	1.23	0.56	0.59	0.84	1.51	1.31	1.24	1.09	0.75	0.82	0.64	0.68	0.80	0.78
Gd	2.68	3.93	2.53	3.56	3.08	4.31	3.35	4.19	4.80	3.10	2.30	3.42	3.06	3.29	3.01
Tb	0.98	0.65	0.58	—	—	0.66	0.45	0.68	0.84	0.58	0.41	0.49	0.82	0.70	0.60
Dy	—	—	—	3.27	3.03	—	—	—	—	2.73	1.83	2.51	—	—	—
Tm	0.36	0.22	0.23	—	—	0.17	0.12	0.27	0.30	0.34	0.25	0.30	0.43	0.48	0.39
Yb	2.31	1.10	1.39	2.08	1.83	0.97	0.60	1.27	1.90	1.81	1.18	1.31	2.69	3.16	2.45
Lu	0.30	0.10	0.21	0.32	0.30	0.13	0.05	0.17	0.28	0.27	0.19	0.20	0.39	0.45	0.33
Eu/Eu*	0.27	0.72	0.51	0.48	0.73	0.84	0.97	0.89	0.69	0.65	0.86	0.57	0.55	0.73	0.78
(Ce/Yb)N	10.7	34.6	13.5	8.2	10.1	25.4	73.3	13.5	10.2	9.8	7.5	9.7	7.1	6.3	13.4

Eu*: Eu value derived by interpolation between Sm and Gd.

N : Chondrite normalized value. +: analysed by ICP.

Numbers in parentheses show the numbers of samples analyzed.

Data of JB after Seo (1985), and CM, CJ and CB after Tsusue et al (1984).

formation of crystallization by the composition of CIPW norm plot on the Q-Or-Ab diagram (Hong, 1985b); (6) The evolved patterns of the granite gneiss in the major element illustrate that they could be generated *either* by low degree of partial melting *or* by high degree of fractionation; (7) The K/Rb ratio shows no significant variations of 93-147 with an average ratio of 123; (8) High Rb/Sr ratio (4.1) can be explained by *either* strong fractionation of magma *or* low degree of partial melting in the source region: the latter is favoured with chemical evidences of small variations in major element, varying incompatible element contents and constantly low concentrations of compatible elements (Fig. 3); (9) The granite protolith (about 2.1 Ga) metamorphosed to form the granite gneiss.

A multi-element mantle-normalized diagram (Fig. 3) serves to summarize the relative distribution and behaviour of different groups of

incompatible elements, emphasising in particular the difference between the large ion lithophile

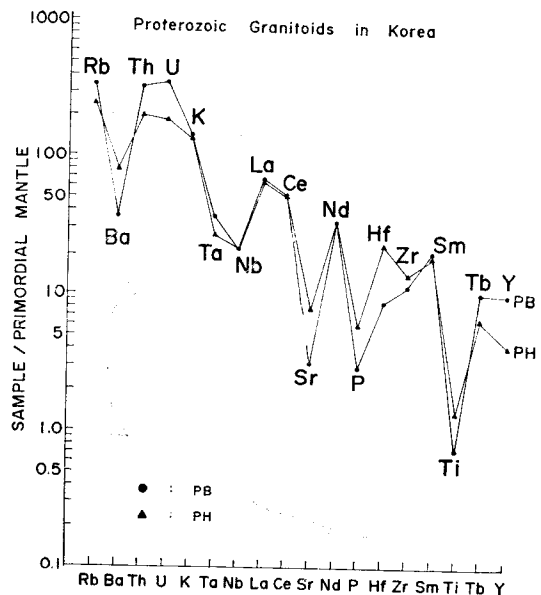


Fig. 3 Distribution of primordial mantle-normalized trace element contents for the Proterozoic granitoids.

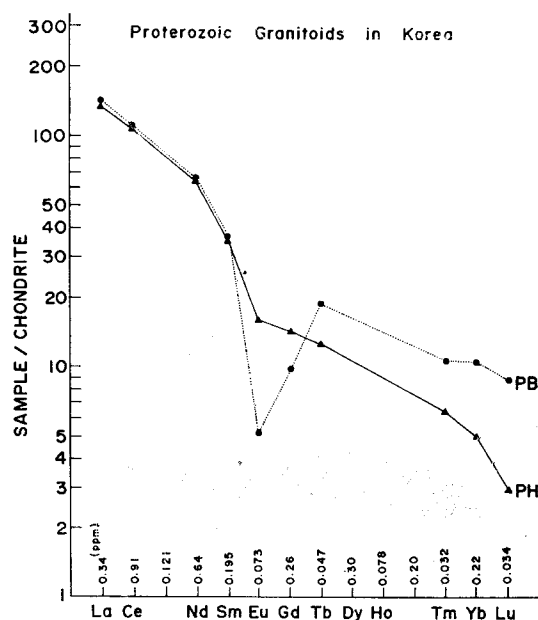


Fig. 4 Chondrite-normalized REE patterns for the Proterozoic granitoids.

(LIL) elements and highly charged high field strength (HFS) elements with small ionic radii (Brown et al., 1984). In overall, the granite gneiss shows high content of the incompatible elements (K, Rb, Th, U) and low concentration in the less mobile elements such as Sr, P and Ti (Fig. 3). The rare earth element (REE) data are presented in Table 7 and are further displayed as chondrite-normalized (Wood, 1979) pattern in Fig. 4. The REE pattern of the granite gneiss shows light REE enrichment and heavy REE depletion with chondrite normalized (Ce/Yb) value of 11. All the REE patterns having pronounced Eu negative anomalies with Eu/Eu^* of 0.24–0.32 and lower Sr content (72ppm) indicate the derivation from plagioclase-depleted source region or the retention of plagioclase, which has high partition coefficients for Sr, Eu and K/Rb (Arth, 1979), in the residuum during partial melting: the most of plagioclase crystals were not melted from a protolith due to low degree of partial melting. The REE patterns, low $^{87}\text{Sr}/^{86}\text{Sr}$ initial ratios (0.7056~

0.7082), Sr, Eu and K/Rb, and high Rb/Sr and differentiation indices imply that the granite gneiss probably produced from I-type plagioclase depleted igneous source rocks (such as granitic compositions).

The Proterozoic granite (PH) presents: (1) A wide range of compositional variations in SiO_2 (67.44~74.73%), MgO, CaO and FeO(t) contents; (2) The $\text{K}_2\text{O}/\text{Na}_2\text{O}$ ratios from 0.70 to 3.46 with an average of 1.59; (3) The normative corundum and molecular $\text{Al}_2\text{O}_3/(\text{Na}_2\text{O} + \text{K}_2\text{O} + \text{CaO})$ ratio are $2.45 \pm 1.12\%$ and 1.11, respectively; (4) The linear trends of major element indicate *either* progressive separation of residuum (restite)–melt during partial melting *or* fractional crystallization from magmatic liquid; (5) Large variation in K/Rb ratios ranging widely from 106 to 261 with a mean of 167 and low Rb/Sr (1.2); (6) The mantle-normalized patterns exhibit LIL element enrichment, although the abundances of several elements notably Sr, P, Ti, Ta and Nb decrease with increasing evolution of the melt (Fig. 3); (7) Strongly fractionated REE patterns with a significant heavy REE depletion and light REE enrichment with chondrite normalized (Ce/Yb) value of 35 (Fig. 4). In particular, their high chondrite normalized (Ce/Yb) ratios suggest the granite contains a substantial proportion of material derived from the reworking of sialic crust. The high fractionated REE pattern, mild Eu negative anomalies (0.59~0.87) and high Sr content (178ppm) postulate a high degree of partial melting involving plagioclase. Most of hornblende and garnet, which have high heavy REE contents, may be left in the residue, but the plagioclase crystals melted to form a granitic magma during the process of partial melting; (8) The high chondrite normalized REE patterns and small Eu anomalies in the granites agree with the REE patterns in the Precambrian sedimentary rocks of the

Canadian Shield (Shaw et al., 1976); (9) High initial $^{87}\text{Sr}/^{86}\text{Sr}$ ratio (0.717~0.723) and peraluminous as mol $\text{Al}_2\text{O}_3/(\text{Na}_2\text{O}+\text{K}_2\text{O}+\text{CaO})$ ratios greater than 1.05 are therefore characteristics of granitoid derived from a sedimentary source; (10) The Proterozoic granite is suggested to be formed by partial melting of the sedimentary rocks (S-type).

The Jurassic Granites

The Jurassic granites can be further divided into cratonic (Gyeonggi massif) and mobile belt (Ogcheon Fold Belt) granites by regional distribution and geochemical distinctions (Fig. 1).

The cratonic granites (JS, JB, and JC) in the Gyeonggi massif show: (1) The silica content ranges from 70% to 76% with a little variation; (2) The granites are positioned toward the alkali side with a small scatter on AFM diagram (Fig. 2); (3) Plot of normative proportion of Q-Ab-Or illustrates a relatively tight group with very little scatter and lies near the thermal minima (Hong, 1984 b; Seo, 1985; Jin et al., 1986); (4) High concentrations of Rb, Th, U and K, and low Sr, Zr and Ti contents; (5) The high Rb/Sr (1.4) and initial $^{87}\text{Sr}/^{86}\text{Sr}$ ratio (0.712~0.715), and low K/Rb and HFS elements make it unlikely a genetic model such as fractional crystallization of direct mantle-derived rocks; (6) The primordial mantle normalized patterns (Fig. 5) for the Jurassic cratonic and mobile belt granites are chemically similar in general: the former has higher incompatible elements (Rb, Th, U, K) and lower Sr content relative to the latter; (7) The REE patterns (Fig. 6) for the cratonic granites show light REE enrichment a little depletion of heavy REE (chondrite normalized Ce/Yb ratio is about 11) with Eu negative anomalies ($\text{Eu}/\text{Eu}^*=0.51\sim 0.73$); (8) The marked Eu anomaly and the low concentrations of Sr in the granites indicate that plagioclase played an important role as a residual phase during melting or fractional crystallization;

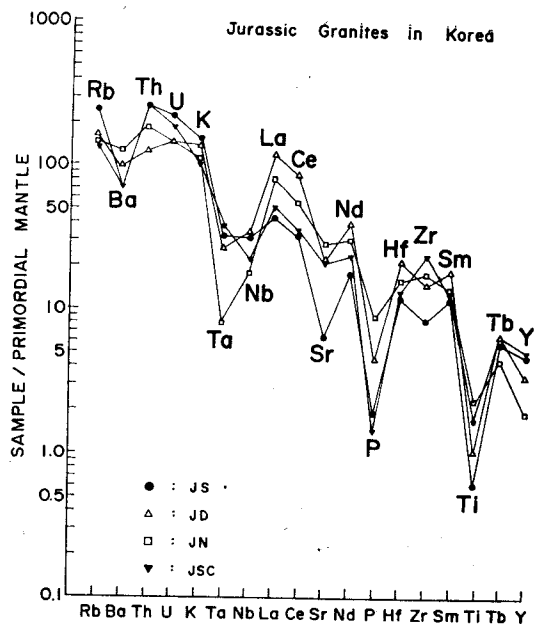


Fig. 5 Primordial mantle-normalized trace element patterns of the Jurassic granites.

(9) The high Rb of the cratonic granites suggests derivation from a parent which was not depleted in Rb, which agrees also with high $\text{K}_2\text{O}/\text{Na}_2\text{O}$ (1.15), therefore, granulite facies rocks, which have low K and Rb contents, are ruled out as a parent being already depleted in Th, U, K and Rb (Heier, 1973); (10) The cratonic granites may have been derived more likely from low to medium grade metasedimentary basement rocks rather than granulite facies rocks, since the granites contain high content of heat producing elements such as Th, U, K and Rb (Fig. 5); (11) Differences in the REE patterns of the cratonic granites in the Gyeonggi massif and the mobile belt granites in the Ogcheon Fold Belt (Fig. 6) could have resulted from source materials of variable compositions and/or from different physical conditions (e.g. oxygen fugacity) for the emplacement of the magmas. Heavy REE (HREE) enrichment in the cratonic granites may be dependent on the amount of garnet (and hornblende) left in the residue. If the cratonic and mobile belt granites

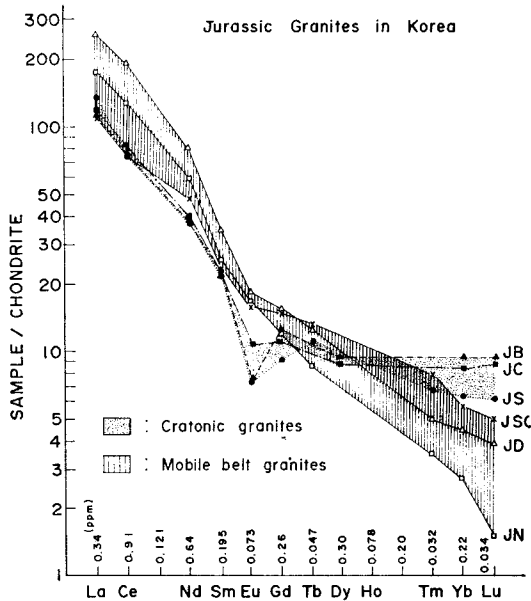


Fig. 6 Chondrite-normalized REE patterns for the Jurassic granites.

were assumed to be derived from similar chemistry of the parental magma; the former granites have undergone advanced fractionation of feldspars compare to the latter (Fig. 6), which is reflected in the large Eu anomalies and HREE enrichment.

The mobile belt granites (JD, JN and JSC) in the Ogcheon Fold Belt have geochemical characteristics as follows: (1) The changes in the abundance of major element show widely scattered in silica content from 63% to 72% in weight; (2) The average ratio of K_2O/Na_2O ranges from 0.83~1.07; (3) High normative corundum, muscovite, and molar proportions of Al_2O_3 in excess of Na_2O+K_2O+CaO reflect peraluminous characters; (4) The primordial mantle-normalized patterns show a similar trend with the cratonic granite in the Gyeonggi massif such as enhanced in Rb, Th, U, K, La and Ce, and depleted in Ta, Nb, P and Ti (Fig. 5); (5) The granites in the Ogcheon Fold Belt show very similar REE patterns with each other (Fig.

6); (6) Strong enrichment in LREE relative to HREE with steep slope with average chondrite normalized ratio being 32.5; (7) They present no significant Eu anomalies ($Eu/Eu^*=0.91$); (8) Strongly fractionated REE patterns with the small or absence of Eu anomaly and high initial $^{87}Sr/^{86}Sr$ ratios of 0.71074~0.7176 are chemically similar to the Precambrian metasedimentary rocks (Shaw et al., 1976). Hornblende fractionation or residual phase of hornblende could account for the pattern of REE distribution and low Rb/Sr (0.2~0.3) in the mobile belt granites, the important feature of hornblende being the high partition coefficient for HREE and the fact that hornblende develops a negative Eu anomaly in equilibrium with silicic liquids (Arth and Barker, 1976). Thus, extensive hornblende fractionation or residual hornblende should yield residual liquids with HREE depletion and positive Eu anomalies. Garnet, also, is potentially capable of reproducing the same REE features (Hanson, 1978); (9) Depletion of HREE in the granites is possibly due to either hornblende and garnet fractionation or those minerals are not involved in the process of partial melting; (10) Large depletion of HREE and Y, and high Sr, CaO and Al_2O_3 in the granites are similar to an Archaean basement rock such as grey gneisses (Martin et al., 1983). The chemical characteristics of such a crustal component would include low Na_2O , K/Rb, HREE, Y and Zr, and high Sr. Most Archaean gneisses clearly have high Ce/Y ratio (Tarney and Windley, 1977); (11) The heat source to melt the large extent of the Precambrian metasedimentary rocks in which Ca and Sr-enriched plagioclases abundant for the mobile belt granites was easily available from the closing the Ogcheon basin together with the basement reactivation during micro-continental collision from which sufficient water provided by the dehydration of the hydrous minerals.

The Cretaceous Granites

The Cretaceous granites in the Gyeongsang basin (CM, CJ, CB, CP, CE and CY) and the Ogcheon Fold Belt (CI) show (Fig. 1): (1) The granites range in composition from intermediate to acid, and produce compositionally expanded calcalkaline trend on AFM diagram (Jin, 1980; 1981); (2) The granites appear to show increase in SiO_2 , K_2O and differentiation index, and decrease total iron, Na_2O , MnO , TiO_2 , MgO , Al_2O_3 , P_2O_5 and CaO ; (3) The decrease of TiO_2 with increasing SiO_2 is usually attributed to the removal of titanomagnetite and ilmenite during fractional crystallization (Saunders et al., 1980); (4) The phase relationship in Or-Ab-An ternary feldspars from the granites lie on the Or-Ab line with variation in An, indicating that the removal of plagioclase from a parental magma will produce a successively more granitic liquid (Jin, 1981; Hong, 1983a); (5) Majority of the granites exhibits mol $\text{Al}_2\text{O}_3 / (\text{Na}_2\text{O} + \text{K}_2\text{O} + \text{CaO})$ values less than 1.05 and normative corundum contents with consistently lower than 1%; (6) Primordial mantle normal-

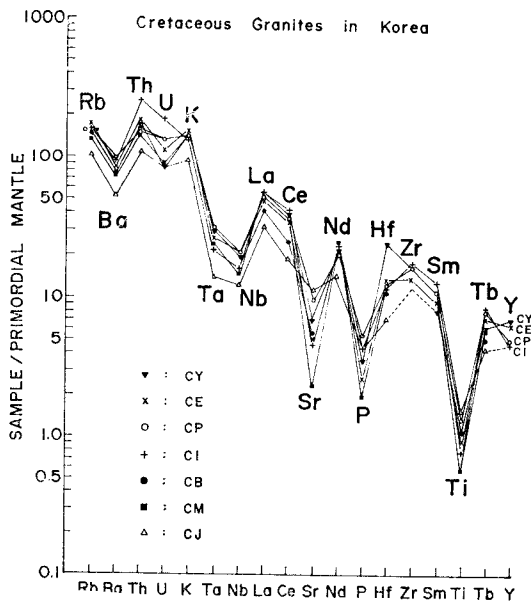


Fig. 7 Primordial mantle-normalized trace elements of the Cretaceous granites.

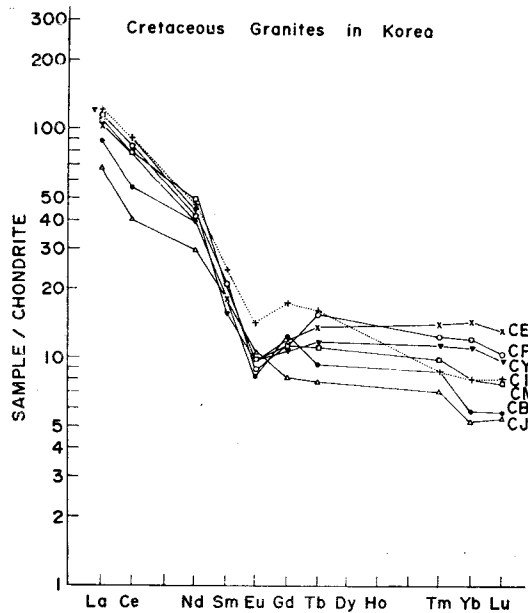


Fig. 8 Chondrite-normalized REE patterns for the Cretaceous granites.

ized patterns for the granites reveals that they are characterized by strong enrichment of Rb, Th, K, La, Ce, Zr and Tb relative to Ba, Ta, Nb, Sr, P and Ti (Fig. 7), which are similar with granites in the Normal Continental Arc Granites (Brown et al., 1984); (7) The trace element geochemistry of the granites show that Rb and Rb/Sr increase with fractionation while Sr, K/Rb and Ca/Y decrease; (8) The REE patterns show a similar trend (Fig. 8) and present light REE and slight depletion of heavy REE with chondrite normalized (Ce/Yb) ratio of 9; (9) Eu negative anomalies ($\text{Eu}/\text{Eu}^* = 0.55 \sim 0.86$) indicate the influence of feldspar fractionation; (10) The granites show low initial $^{87}\text{Sr}/^{86}\text{Sr}$ ratio of 0.704~0.707; (11) The Cretaceous granite in the NE part of the Ogcheon Fold Belt (e.g. CI in Fig. 1) in which Paleozoic carbonaceous formations are predominant shows a different REE patterns with the granites in the Gyeongsang basin. The explanation for the differences in REE patterns is either the granites in the Gyeongsang basin

were undergone more fractionation than in the Ogcheon Fold Belt or the parental magma for the granite in the NE side of the Ogcheon Fold Belt might had been reduced (low oxygen fugacity) owing to contamination of the carbonaceous country rocks; (12) The Cretaceous granites show characteristics of I-type and magnetite-series, and were mainly formed by fractional crystallization of parental magmas (Jin, 1980; 1981, Hong, 1983b; 1985a).

SUMMARY AND TECTONIC SETTING

The granites in Korea display distinctive petrological and geochemical characteristics (Table 8 and Fig. 9) showing that the parental magmas and their evolutionary paths were also distinct. This section sets out to summarize the contrasting geochemical characteristics, in particular trace element, of the granites and to define the general environment in which they were emplaced. Further, an attempt is made to produce a possible tectonic evolution model for the generation of the granitic rocks of Korean peninsula. The conclusions on the origin and crystallization

process of the studied granites can be summarized briefly as follows:

The Proterozoic Granitoids: The Proterozoic granite gneiss (I-type) probably formed by metamorphism of rather geochemically evolved igneous rocks such as I-type granitic rocks in which the plagioclases were already depleted due to low degree of partial melting with geochemical evidences such as high chondrite-normalized (Ce/Yb) ratio of 11 and incompatible element, large negative Eu anomalies (0.24~0.32), low initial ⁸⁷Sr/⁸⁶Sr ratios of 0.7056~0.7082 and compatible element.

The considerable variations of major and trace elements, very high chondrite-normalized (Ce/Yb) ratios of 35 small negative Eu anomalies (0.59~0.87) and high ⁸⁷Sr/⁸⁶Sr initial ratios (0.717~0.723) in the Proterozoic granite (S-type) that the granite may be produced by remobilization of sialic crust; probably a function of progressive high degree of partial melting of immature sedimentary rocks (e.g. greywacke-rich rocks). The small temperature variations (±20°C) of the perthites in the (PH) could be explained as the country rocks adjacent to the granite had been under high heat flow regime during the intrusion and those rocks had cooled down slowly. The high Precambrian geothermal gradients make it likely to bring the large-scale crustal remelting.

The Jurassic Granites: High value of the initial Sr ratios (0.711~0.718) of Jurassic granites together with an average of more than 1% corundum (0.57~1.35%) in norm would suggest the derivation of the granites from crustal materials, possibly metasedimentary rocks.

The S-type Jurassic granites can be further divided into cratonic (Gyeonggi massif) and mobile belt (Ogcheon Fold Belt) granites (Fig. 1). High normative anorthite and K/Rb, and lower Rb/Sr and D.I in the mobile belt granites

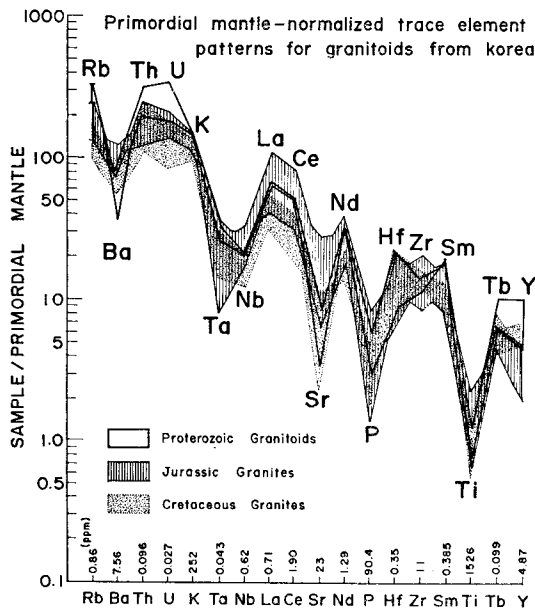


Fig. 9 Primordial mantle-normalized trace element patterns for the granitoids in Korea.

Table 8 Comparison of geochemical characteristics of the granites in Korea.

KEY	Proterozoic (PB & PH)	Jurassic		Cretaceous (CI, CM, CJ, CB, CP, CE & CY)
		Cratonic (JS, JB & JC)	Mobile belt (JSC, JN & JD)	
Classification	"I-type" alkaline granite gneiss (PB) and "S-type" calc-alkaline granite (PH)	"S-type" subsolvus alkaline monzogranite	"S-type" subsolvus calcalkaline granodiorite (JSC, JN) and monzogranite (JD)	"I-type" subsolvus calcalkaline monzogranite
Age	2100Ma (PB), 1700Ma (PH)	160±10Ma	153~167Ma (JN) 190Ma (JD)	72~87 Ma, 97 Ma (CI)
Lithology of envelope (contacts)	PC clastic sedimentary rocks and Paleozoic carbonates (PB: sharp, PH: concordant)	PC gneiss (sharp)	PC gneiss & marine sedimentary rocks (rather concordant)	Cretaceous andesites & non-marine sedimentary rocks (sharp)
Occurrence	Batholith	Batholith (NE-SW direction)	Batholith (NE-SW direction)	Oval and irregular stocks
Texture	Equigranular & porphyroblastic	Equigranular (and hypidiomorphic)	JSC (porphyroclastic), JN (porphyroblastic) & JD (equigranular) with strong foliation	Porphyritic
Mineralogical distinction	Microcline, biotite, oligoclase (PB), microcline, two-mica, garnet, tourmaline (PH)	Myrmekite, microcline, perthite & undulose strained quartz	Myrmekite, microcline, perthite, muscovite, sphene & undulose strained quartz	Microperthite, hornblende, tourmaline & allanite, interstitial micrographic quartz
Differentiation Index	87 (PB) & 83 (PH)	85~92	73~82	75~91
K ₂ O/Na ₂ O (K/Rb)	1.43 (PB) & 1.59 (PH) (123~167)	1.15(183)	0.83~1.07 (220~229)	1.05~1.12 (242~292)
Normative corundum	1.27 (PB) & 2.45 (PH)	0.57~1.35	0.70~1.33	0.20~0.94
Rb/Sr ratio	4.1 (PB) & 1.2 (PH)	1.4~0.5	0.2 (JSC, JN) & 0.3 (JD)	0.3~2.1
Total REE content	199ppm (PB) & 195ppm (PH)	124ppm	145ppm (JSC), 251ppm (JN & JD)	143~156 ppm
Eu/Eu*	0.24~0.32 (PB), 0.59~0.87 (PH)	0.51~0.73	0.84~0.97	0.55~0.86
Oxygen fugacity	large (PB), small (PH)	large	small	large
(Ce/Yb) N	11 (PB) & 35 (PH)	11	19 & 73 (JN)	9
Emplacement	Mesozone (PB), Kata or Mesozone (PH)	Mesozone	Kata or Mesozone	Epizone
Perthite exsolution T°C	330±20 (PH)	315±20	430±30	520±110
Magma cooling	Slow	Slow	Slow	Rapid
H ₂ O in primary magma	Dry (PB), Wet (PH)	Wet	Wet	Dry
(⁸⁷ Sr/ ⁸⁶ Sr) Initial ratio	0.7056~0.7082 (PB), 0.7174~0.7229 (PH)	0.712~0.715	0.711~0.718	0.704~0.707

Ore mineralisation associated with granite	—	—	Au-Ag-CaF ₂ in Quartz vein	Pb-Zn-Au-Mo-W polymetallic (Andean-type)
Tectonism & probable crustal thickness	—	Late-tectonic & thick crust	Syntectonic (Hercynotype) & thin crust	Post-tectonic (Adnino-type) & thick crust
Petrogenetic process	Partial melting	Partial melting	Partial melting	Fractional crystallization

can be explained by the cratonic granites being more evolved *either* during intrusion through thick crust *or* owing to lower degree of partial melting. The mobile belt granites show the characteristics of very small negative Eu anomaly ($\text{Eu}/\text{Eu}^*=0.90$), depleted HREE and high total REE content (145~251ppm), whereas the cratonic granites have Eu negative anomaly ($\text{Eu}/\text{Eu}^*=0.51\sim 0.73$) and total REE content of 124 ppm. The different features of the geochemistry between the mobile belt and cratonic granites are considered to be mainly due to different proportion of partial melting according to trace element modelling: If geochemically similar source regions are assumed, the mobile belt granites are thought to have been derived from higher degree of partial melting than the cratonic granites (Hong, 1983).

The low temperatures (315~430°C) and small temperature variations ($\pm 30^\circ\text{C}$) in cessation of exsolution of perthites for the Jurassic granites might have been caused by the country rocks around the granites under regional metamorphic regime and cooled down slowly. The slow cooling of magma in the high heat flow area could not form a kind of solidified shell in the outer part of the intruded mass (impermeable shell). Therefore, the aqueous vapour phase which transport the metallic ions in the magma could escape and disperse into the surrounding rocks, that is one of the reasons for absence of metallic ore deposits associated with the Jurassic granites.

The Cretaceous Granites: The Cretaceous

granites are almost porphyritic in texture, or occasionally uneven in grain size, ranging from fine to medium, inward from the margin. Microclines are abundant in the Jurassic granites, whilst orthoclase occurs in the Cretaceous granites; which indicates that the former crystallized slowly at low temperature (deep seated), whilst the latter solidified more rapidly at higher temperatures. The rapid cooling of magma provoked the formation of a kind of solidified shell in the outer part of the pluton. The shell is impermeable and hence the retention of the aqueous vapour phase. The contents of the volatile transport such as chlorine in the apatite and biotite are higher from the Cretaceous granites relative to the Jurassic ones (Tsusue et al., 1981).

The Cretaceous granites range in composition from intermediate to acid, and produce compositionally expanded calcalkaline trends in major and trace elements. Analytical results of perthitic alkali-feldspars from the granites show that the average temperature of cessation of exsolution was about $520\pm 110^\circ\text{C}$ at assumed pressures. The large range of temperature variation ($\pm 110^\circ\text{C}$) of the perthites in each granite body is consistent with the interpretation that the granites were solidified from margins to inwards with rather stable magmatic conditions (post-tectonic anhydrous magma). The trace element geochemistry of the granites show that Rb and Rb/Sr increase with fractionation while Sr, K/Rb and Ce/Y decrease. The REE patterns present light REE and slight depletion of heavy

REE with chondrite-normalized (Ce/Yb) ratio of 9. The Eu negative anomalies ($\text{Eu}/\text{Eu}^* = 0.55 \sim 0.86$) indicate the influence of feldspar fractionation. Low initial $^{87}\text{Sr}/^{86}\text{Sr}$ ratio of $0.704 \sim 0.707$ denotes that their magmas were essentially derived from the igneous protolith (I-type) in the lower crust and/or upper mantle.

Rare Earth Elements in the Granites

Minor and trace elements are better indicators of magmatic evolution than major elements, as they are more sensitive to changing conditions of partial melting and fractional crystallization, and source composition. Data on partitioning of the rare earth elements (REE) promise to be particularly useful because these trace elements constitute a chemically coherent group having notably the small decrease in ionic radius with increase in atomic number. The REE abundance data for the Korean granites have been normalized to the average chondritic contents (Wood, 1979), and on a logarithmic scale against atomic numbers (Figs. 4, 6 and 8), which illustrate quite different REE patterns among the studied granites in different time and space.

The Proterozoic granites also show distinctly different REE patterns (Fig. 4). The REE pattern of the Buncheon granite gneiss (PB) show light REE enrichment and heavy REE depletion with (Ce/Yb) N of 10.7 and have large Eu negative anomalies with Eu/Eu^* of 0.27. The Hongjesa granite (PH) shows strongly fractionated REE patterns with a significantly heavy REE depletion and light REE enrichment with (Ce/Yb)N ratio of 34.6, and presents a mild Eu negative anomaly ($\text{Eu}/\text{Eu}^* = 0.72$).

The REE abundance data illustrate different REE patterns (Fig. 6) between the Jurassic granites in the Gyeonggi massif (cratonic) and in the Ogcheon Fold Belt (mobile belt). The REE patterns for the Jurassic granites in the Ogcheon Fold Belt yield very similar patterns with steep negative slopes, light REE

enrichment and heavy REE depletion with an average chondrite normalized (Ce/Yb) ratio of 32.5, and a very small or absent Eu anomalies. But, the REE patterns for the granites in the Gyeonggi massif show light REE enrichment and a little depletion of heavy REE (Ce/Yb) N=11 with Eu negative anomalies ($\text{Eu}/\text{Eu}^* = 0.51 \sim 0.73$).

The Cretaceous granites in the Gyeongsang basin illustrate a similar trend (Fig. 8) and present light REE and slight depletion of heavy REE (Ce/Yb)N=9 with Eu negative anomalies ($\text{Eu}/\text{Eu}^* = 0.55 \sim 0.86$). The Cretaceous granite in the NE part of the Ogcheon Fold Belt (CI) present light REE enrichment and heavy REE depletion with (Ce/Yb)N ratio of 10.2 and have moderate negative Eu anomalies ($\text{Eu}/\text{Eu}^* = 0.69$). The chondrite normalized REE patterns for the Mesozoic granites in Korea present a quite different distribution (Fig. 10):

- 1) The Jurassic granites in the Ogcheon Fold Belt with large (LREE/HREE) ratios and with very mild negative Eu anomalies;
- 2) The Cretaceous granites in the Gyeongsang basin with small (LREE/HREE) ratios and with negative Eu anomalies.

The partition of Eu between plagioclase and magmatic liquid is a strong function of oxygen fugacity (Drake and Weill, 1975; Sun et al., 1974). Several of the REE exhibit exceptional behaviour under certain physical conditions because they have significant stabilities in valence state other than +3. The most striking exceptional behaviour is displayed by Eu, which stable both divalent and trivalent states at magmatic redox conditions. The striking effect of variations in temperature and oxygen fugacity on the measured or effective plagioclase/liquid distribution coefficient for Eu suggests that $\text{Eu}^{+2}/\text{Eu}^{+3}$ ratios in rock-forming phases may be used to estimate oxygen fugacities.

Existing analytical techniques do not permit

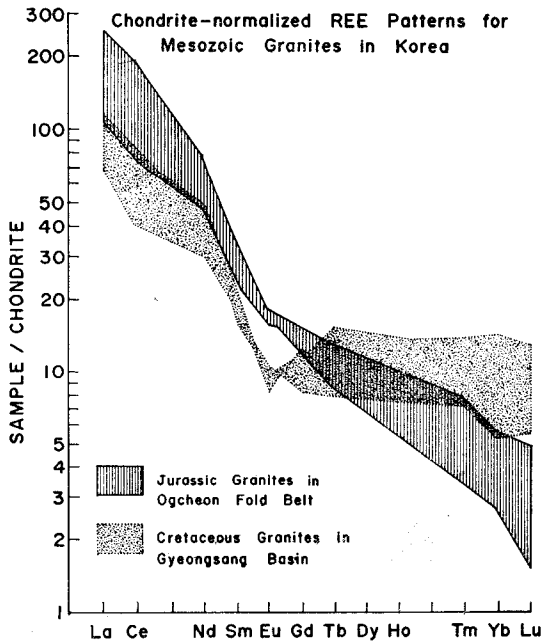


Fig. 10 Chondrite-normalized REE patterns for Mesozoic granites in Korea.

the direct measurement of Eu^{+2} (which is similar with Sr^{+2} in ionic charge and radius) and Eu^{+3} in most natural phases. As most of the REE are stable only in the trivalent state distribution coefficient Eu^{+3} may be obtained by interpolating a smooth REE pattern versus ionic radius plot at the Eu position. The steep negative slope without Eu anomaly in the Jurassic granites (Fig. 10) can be explained as fractionation of Eu^{+2} in plagioclase is prevented by low oxygen fugacity (f_{O_2}) condition in the parental magma and/or partial melting carbon rich sedimentary rocks. In reducing condition, the distribution coefficient (D) of Sr^{+2} and Eu^{+2} in the plagioclase is low. The small LREE/HREE ratios with negative Eu anomalies in the Cretaceous granites imply that the rocks crystallized in the high f_{O_2} condition. In the oxidation condition, Eu^{+2} is rather unstable than Eu^{+3} and D of Eu^{+2} in plagioclase also high.

Differences in the REE patterns of the cratonic and mobile belt granites (Fig. 6) could have

resulted from source materials of variable composition for the generation of the magmas or the cratonic granites have undergone advanced fractionation of feldspars compare to the mobile granites. The Proterozoic granitoids also illustrate different REE patterns (Fig. 4); the REE pattern of the Buncheon granite gneiss is rather similar to the Cretaceous granites in the Gyeongsang Basin: the Hongjesa granite resembles to the Jurassic granites in the Ogcheon Fold Belt in REE pattern.

In terms of oxygen fugacity during the feldspar crystallization in the granite magmas, the Jurassic granites in the Ogcheon Fold Belt were crystallized in the lowest f_{O_2} condition of the parental magma among the Korean granites, whereas the Cretaceous granites in the Gyeongsang basin at the high f_{O_2} condition. The Jurassic granites in the Gyeonggi massif were crystallized at intermediate f_{O_2} condition relative to the other granites from the Ogcheon Fold Belt and Gyeongsang basin.

Tectonic Setting of the Mesozoic Granites

Granites may be subdivided according to their intrusive setting into four main groups (Pearce et al., 1984) ocean ridge granites (ORG), volcanic arc granites (VAG), within plate granites (WPG) and collision granites (Syn-COLG). Discrimination of ORG, VAG, WPG and syn-COLG is most effective on projection of Nb–Y, Rb–(Yb+Ta) and Ta–Yb. Geochemical characteristics such as trace element compositions in granites can clearly help in the elucidation of post-Cambrian tectonic settings. On the Nb–Y, Ta–Yb and Rb–(Yb+Ta) discriminant diagrams, the Jurassic granites in Korea mainly straddle the compositional field of “syn-collisional” granite whereas the Cretaceous granites lie in the region of the “volcanic arc” granite (Figs. 11, 12 and 13).

The mode of the formation of the Ogcheon

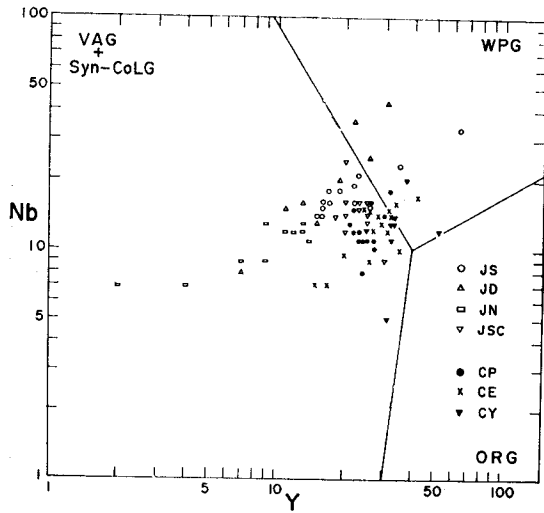


Fig. 11 Nb versus Y discriminant diagram (after Pearce et al., 1984) for the Mesozoic granites.

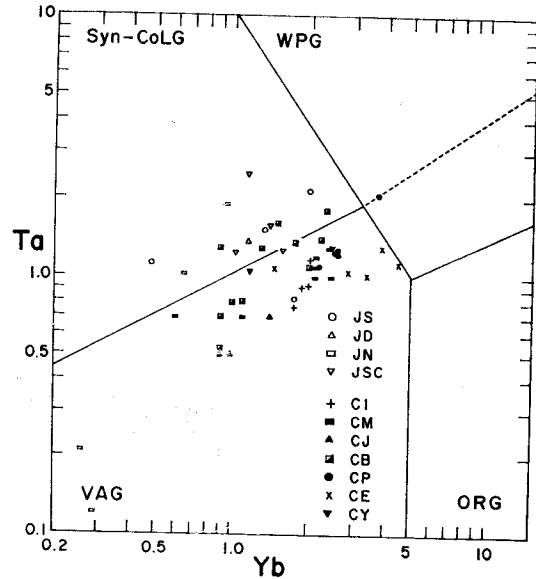


Fig. 13 Ta versus Yb discriminant diagram (after Pearce et al., 1984) for the Mesozoic granites.

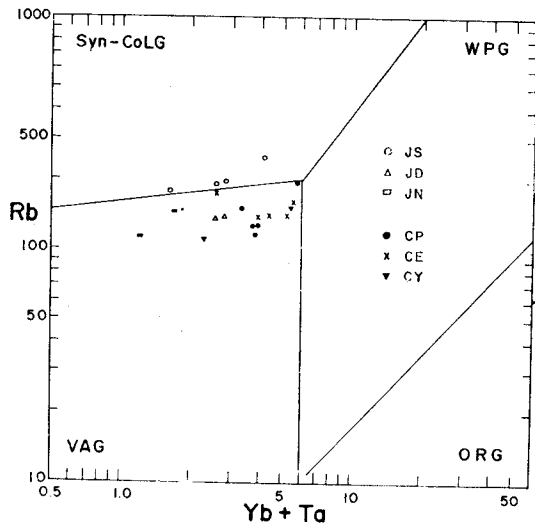


Fig. 12 Rb versus Yb+Ta discriminant diagram (after Pearce et al., 1984) for the Mesozoic granites.

Fold Belt, where the Jurassic granitic rocks are dominantly distributed, is vital to the understanding of the tectonic evolution of the Korean peninsula (Fig. 1). Some geologists were tempted to interpret the resulting Fold Belt as having been formed by: (1) Collision of continental fragments of micro-plates (Sillitoe, 1975); (2) In relation to the presence of a convergent plate margin in the vicinity of Japan (Park

and So, 1973); (3) The movement of basement blocks in the intracratonic sedimentary basin (Reedman and Um, 1975; Fletcher, 1976); and (4) Mantle hot spots or thermal rises model (Park and Do, 1974; Workman, 1972).

The Jurassic granites are dominant at the Ogcheon Fold Belt (a Hercynotype Fold Belt), resulting perhaps by closing-collision situation such as compressional tectonic setting (Fig. 14 b). Shortening of the crust leads to tectonic thickening when, particularly as a consequence of uplift, magmas are generated within the regionally heated root. It is in this context that crustal-derived "S-type" granitic magmas are most likely to occur, and be emplaced into a ductile crust. The Jurassic granites in the Ogcheon Fold Belt may reflect a relaxation process after extreme thickening of continental crust following continental collision (with basement block movement). According to currently accepted plate tectonic theory, such collision can occur if an ocean or a marginal basin closes, and such collision can occur by the process of sea-floor spreading of oceanic lithosphere. In

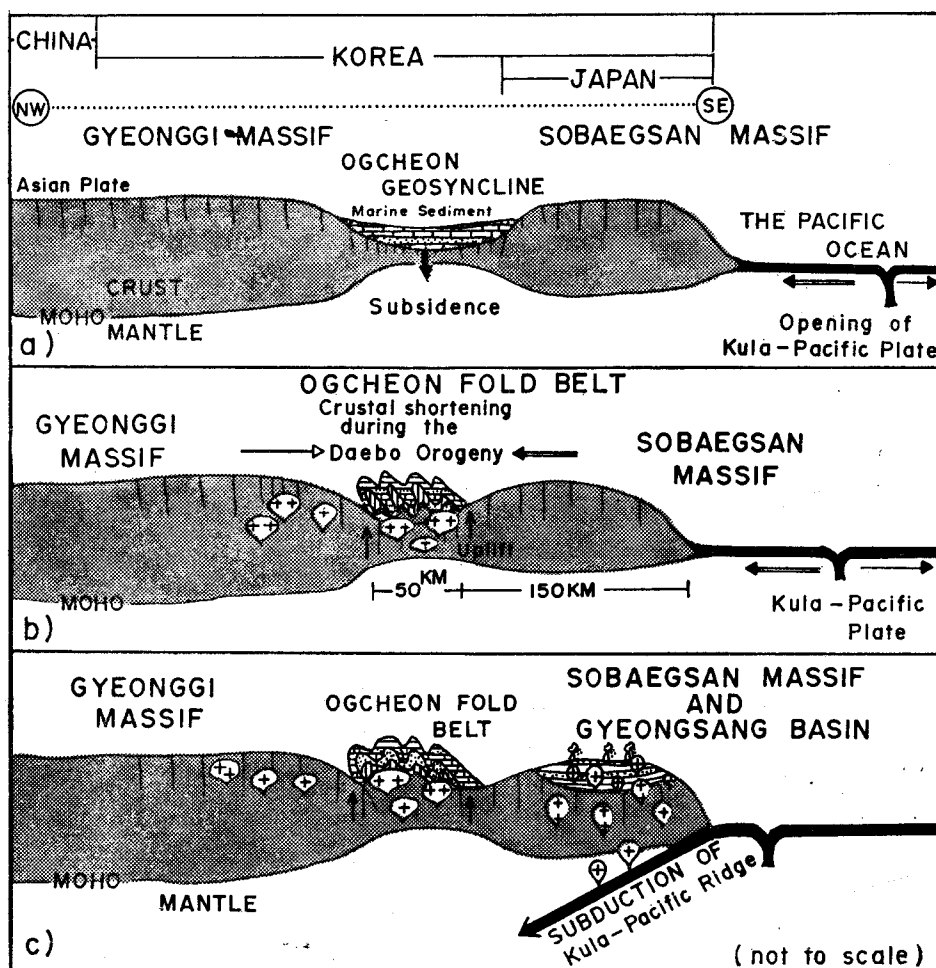


Fig. 14a Schematic diagram for the tectonic evolution of Korean peninsula until late Paleozoic. The vertical lines are deep fractures along the Sinian direction.

14b Schematic diagram of the closing (and collision) of the Ogcheon Fold Belt in early to middle Jurassic.

14c Schematic diagram of the subduction of the Kula-Pacific ridge and igneous activity in a marginal basin during Cretaceous-Tertiary.

contrast, beneath a continental margin of Andino-type, which is possibly comparable with the Cretaceous—Tertiary granites in Korea, subduction energetics provide sufficient heat and water to trigger remelting at various subcrustal and lower crustal levels (Fig. 14c). By such means, material continuously accreting beneath the continental edge is episodically remobilized (during periods of subduction) by hot basic magmas that melt their way up into the crust along deep-reaching crustal fractures (e. g. these of Sinian direction).

These "I-type" magmas are permissively accepted by the rigid crust at higher levels in the form of cauldrons and to form granitic bodies. In late Early Cretaceous times, SE Korea was involved in block-movements and concomitant volcanic eruptions, which is the early phase of extensional tectonics that dominated in Korea and the surrounding areas in Cretaceous and Cenozoic times (Chang, 1975; 1978). The later stage of the Gyeongsang basin development was characterised by a culmination of volcanism,

and the termination of the basin development was coincident with the emplacement of granites in the Late Cretaceous, intruded at a shallow crustal level. The early volcanism produced largely basaltic lava, and the compositions of the succeeding lavas became more acidic towards the top to the Gyeongsang sequence. Usually, subsidence was facilitated by pre-existing faults; thus, some depressions are rectangular in outline, being inserted between two sets of faults perpendicular to one another. Typical cauldron subsidence, with ring dikes along ring faults, also occurs. During the Cretaceous times, the Kula oceanic plate was subducted beneath the Asiatic continent at a rate which varied between 16cm/yr and 24cm/yr (Uyeda and Miyashiro 1974), and this was followed by the descent of the Kula-Pacific ridge. It has been postulated that the subduction of this ridge would produce a hot plate with low dip, and therefore would account for the wide zone of magmatism and volcanism found within the Asiatic continent (Uyeda and Miyashiro 1974). A multi-stage model for the generation of the Cretaceous-Tertiary granites in Korea is suggested. The first stage, or trigger mechanism, is the production of basaltic and andesitic magmas from the subduction of the Kula-Pacific ridge. These magmas then migrated upwards, and later reheated the basaltic and andesitic magmas to produce granitic magmas. It is only in the Andinotype context that there is a clear space-time relationship between plutonism and volcanism. To rise at all, the magmas filling the cauldrons, especially the relatively dry magmas of destructive plate margins, need to be channelled and relatively rapidly intruded along major fractures, creating a narrow heat plume within a cool upper crust. Such hot magmas, derived at least in part from the mantle, might have a sufficiently low viscosity, when isolated in their chambers, to permit differentiation in

situ and so provide volcanic derivatives.

CONCLUSIONS

The observations and geochemical arguments presented for the Korean granites lead to the following general conclusions:

1) The granites in Korea can be classified into three different ages of granites with their own distinctive geochemical patterns such as the Proterozoic granitoids, the Jurassic granites (cratonic and mobile belt) and the Cretaceous-Tertiary granites;

2) The Proterozoic granite gneiss (I-type and ilmenite-series) formed by metamorphism of the I-type and rather geochemically evolved granite protolith. The Proterozoic granite (S-type and ilmenite-series) produced by remobilization of sialic crust such as high degree of partial melting of immature sedimentary rocks (e.g. greywacke-rich rocks);

3) The Jurassic granites (S-type and ilmenite-series) were mainly formed by partial melting of crustal materials, possibly metasedimentary rocks. The different features of the geochemistry between the mobile belt and cratonic granites are considered to be due to the different proportions of partial melting and/or of differentiation;

4) The Cretaceous granites (I-type and magnetite-series) formed by fractional crystallization of parental magmas from the igneous protolith in the lower crust and/or upper mantle. The granites were emplaced at high level with a direct link between the plutons and andesitic volcanicity, which is similar to the Andean Cordillera;

5) In terms of oxygen fugacity in the parental magma, the Jurassic mobile belt granites were crystallized in the lowest oxygen fugacity condition among the Korean granites, whereas the Cretaceous granites in the Gyeongsang basin at the highest oxygen fugacity condition. The Jurassic

cratonic granites were crystallized at intermediate oxygen fugacity condition;

6) The granites in Korea belong to the "Normal calc-alkaline continental arc" granitoids on the multi-element mantle normalized diagram suggested by Brown et al. (1984). On the discriminant diagrams for intrusive setting (Pearce et al., 1984), the Jurassic granites mainly straddle the compositional field of "syn-collisional" granite whereas the Cretaceous granites lie in the region of the "volcanic arc" granite;

7) The Jurassic granites are dominant at the Ogcheon Fold Belt (a Hercynotype Fold Belt), resulting perhaps by closing-collision situation such as compressional tectonic setting during the high speed (16~24cm/yr) of sea floor spreading of the Kula-Pacific plate. The crustal-derived S-type granitic magmas are easily to occur by dehydration of mica-rich metasedimentary rocks (wet-magma), and be emplaced into a ductile crust. The Jurassic granites in the Gyeonggi massif might be more evolved *either* during intrusion through thick crust *or* owing to lower degree of partial melting in comparison with the Jurassic mobile belt granites;

8) The Cretaceous-Tertiary granites are possibly comparable with a continental margin of Andinotype, subduction of the Kula-Pacific ridge provide sufficient heat and water to trigger remelting at various subcrustal and lower crustal igneous protoliths. To rise the granitic magmas, the magmas filling the cauldrons, especially the dry magmas of destructive plate margins, need to be channelled and relatively rapidly intruded along major fractures, creating a narrow heat plume within a cool upper crust;

9) The low temperatures (315~430°C) and small temperature variations ($\pm 20^\circ \sim 30^\circ \text{C}$) in the cessation of exsolution of perthites for the Proterozoic and Jurassic granites might have been caused by the country rocks around the granites under high heat flow regime. The high

temperature (520°C) and large variations ($\pm 110^\circ \text{C}$) of perthites for the Cretaceous granites postulate that the rapid cooling of the granitic magmas. The solidified shell in the outer part of the Cretaceous intrusives was rather impermeable and hence the differences in temperature of cessation of perthite exsolution should be large. There might have been temperature differences between the country rocks and granitic magmas such as small difference in the Proterozoic and Jurassic granites, and large in the Cretaceous granites;

10) Extensive and detailed mapping, and geochemical study on the granites in Korea would be worthwhile to reveal more of the internal variations and contact relationships in the different rock types. Accurate and systematic isotope studies might also throw more light on petrogenetic and metallogenetic problems. Vigorous trace element modelling may be a worthwhile exercise in future studies.

ACKNOWLEDGEMENTS

I am grateful to Dr. P.H. Banham in Univ. of London for inspiring suggestions. Special thanks are extended to Dr. G.F. Marriner for the help of XRF and INAA, and to Dr. P.J. Treloar for the use of EPMA in Univ. of Cambridge. Sincere thanks are expressed to Dr. M.S. Jin for useful discussion.

REFERENCES

- Arth, J.G. (1976) Behaviour of trace elements during magmatic processes, a summary of theoretical models and their applications. *J. of Research of the U.S. Geological Survey*, v. 4, p. 41-47.
- Arth, J.G. and Barker, F. (1976) Rare-earth partitioning between hornblende and dacitic liquid and implications for the genesis of trondhjemitic-tonalitic magma. *Geology*, v. 4, p. 534-536.
- Barth, T.F.W. (1962) A final proposal for calculating the mesonorm of metamorphic rocks. *J. Geol.*, v. 70, p. 494-498.

- Barth, T.F.W. (1968) Additional data for the two-feldspar geothermometer. *Lithos*, v. 1, p. 305-306.
- Brown, G.C., Thorpe, R.S. and Webb, P.C. (1984) The geochemical characteristics of granitoids in contrasting arcs and comments on magma sources. *J. Geol. Soc. London*, v. 141, p. 413-426.
- Brown, W.L. and Parsots, I. (1981) Towards a more practical two-feldspar geothermometer. *Contr. Min. Petrol.*, v. 76, p. 369-377.
- Chang, K.H. (1975) Cretaceous stratigraphy, sedimentation and tectonics of southeastern Korea. *J. Geol. Soc. Korea*, v. 13, No. 2, p. 76-90 (in Korean).
- Chang, K.H. (1978) Aspects of Mesozoic and Cenozoic tectonic history of Korea and related regions. *J. Geol. Soc. Korea*, v. 14, No. 1, p. 25-31 (in Korean).
- Choo, S.H. and Lee, D.J. (1980) A Rb/Sr age determination on a Precambrian granite in the Korean peninsula. KIGAM, unpubl.
- Choo, S.H., Jin, M.S., Yun, H.S. and Kim, D.H. (1982) Rb/Sr age determinations on granite gneiss and granite in Seosan, Onjeongri granite, and Mesozoic granites along the East coast, Korean peninsula. Report on Geosci. and Min. Resources, v. 13, p. 193-208 (in Korean).
- Choo, S.H. and Kim, S.J. (1985) A study of Rb-Sr age determinations on the Ryeongnam massif(I) Pyeonghae, Buncheon and Kimcheon granite gneiss and some granites related with the massif. KIER annual report, 85-24, p. 7-39 (in Korean).
- Drake, M.J. and Weill, D.F. (1975) Partition of Sr, Ba, Ca, Y, Eu^{2+} , Eu^{3+} , and other REE between plagioclase feldspar and magmatic liquid: an experimental study. *Geochim. Cosmochim. Acta*, v. 39, p. 669-712.
- Farrar, E., Clark, A.E. and Kim, O.J. (1978) Age of the Sangdong tungsten deposit, Republic of Korea, and its bearing on metallogeny of the southern Korean peninsula. *Econ. Geol.*, v. 73, p. 547-566.
- Ferry, J.M. (1978) Fluid interaction between granite and sediment during metamorphism, South-Central Maine. *Am. J. Sci.*, v. 278, p. 1025-1056.
- Fletcher, C.J.N. (1976) The geological structure of the Ogcheon area, and its relationship to the development of the intercratonic Ogcheon Fold Belt. Anglo-Korean mineral exploration group, Korea Res. Inst. Geosci. and Mineral Resources (KIGAM), 23 pp.
- Hanson, G.N. (1978) The application of trace element to the petrogenesis of igneous rocks of granitic composition. *Earth Plan. Sci. Lett.*, v. 38, p. 26-43.
- Heier, K.S. (1973) Geochemistry of granulite facies rocks and problems of their origin. *Phil. Trans. Roy. Soc. London, A*, v. 273, p. 429-442.
- Hong, Y.K. (1983a) Petrology and geochemistry of Jurassic and Cretaceous granites, South Korea. Unpubl. PhD thesis, Univ. of London, 365 pp.
- Hong, Y.K. (1983b) Petrology and geochemistry of the Cretaceous Palgongsan granite, Southern Korea. *J. Korea Inst. Min. Geol.*, v. 16, No. 2, p. 83-109.
- Hong, Y.K. (1984a) Petrology and geochemistry of Jurassic Daejeon and Nonson granitoids in the Ogcheon Fold Belt, Korea. *J. Korea Inst. Min. Geol.*, v. 17, No. 3, p. 179-195.
- Hong, Y.K. (1984b) Petrology and geochemistry of Jurassic Seoul and Anyang granites, Korea. *J. Geol. Soc. Korea*, v. 20, No. 1, p. 51-71.
- Hong, Y.K. (1985a) Geochemistry of the Cretaceous Eonyang and Yoocheon granites in the Southeastern Korea. *J. Geol. Soc. Korea*, v. 21 No. 2, p. 90-108.
- Hong, Y.K. (1985b) Petrogenesis of the Proterozoic granitic rocks in the Buncheon-Seogpo area, NE Korea. *J. Geol. Soc. Korea*, v. 21, No. 3, p. 196-209.
- Hong, Y.K. (1986) Geochemistry and K-Ar age of the Imog granite at the Southeastern part of the Hambaeg basin, Korea. *J. Korea Inst. Min. Geol.*, v. 19, No. 2, p. 97-107.
- Jin, M.S. (1980) Geological and isotopic contrasts between the Jurassic granites and the Cretaceous granites in Southern Korea. *J. Geol. Soc. Korea*, v. 16, p. 205-215.
- Jin, M.S. (1981) Petrology and geochemistry of the Cretaceous granitic rocks in southern Korea. Unpubl. PhD thesis, Seoul Nat. Univ. 144pp.
- Jin, M.S., Kim, S.Y. and Lee, J.S. (1981) Granitic magmatism and associated mineralization in the Gyeongsang basin, Korea. *Minining Geol.* v. 31, p. 245-260.
- Jin, M.S. (1985) Geochemistry of the Cretaceous to

- early Tertiary granitic rocks in southern Korea. Pt. 1, Major elements geochemistry. *J. Geol. Soc. Korea*, v. 21, p. 297-316.
- Jin, M.S. (1986) Ca, Na, K, Rb, Zr, Nb and Y abundances of the Cretaceous to early Tertiary granitic rocks in southern Korea and their tectonic implications. *Memoirs for Prof. Sang Man Lee's Sixtieth Birthday*, p. 195-209.
- Jin, M.S., Choo, H.S., Kim, S.J. and Hong, Y.K. (1986) A relationship between granite emplacement and the mineralization. KR-86 (B)-10, Ministry of science and Technology, 68pp (in Korean).
- KIER (1981) 1 : 1,000,000 Geological map of Korea. Seoul.
- Kim, D.H., Choo, S.H. and Lee, D.J. (1978) Rb/Sr age of Hongjesa granite distributed in Seogpo-ri area. *Rept. Geosci. and Mineral Resources*, v. 4, p. 83-101 (in Korean).
- Martin, H., Chauvel, C. and Jahn, B.M. (1983) Major and trace element geochemistry and crustal evolution of Archaean granodioritic rocks from Eastern Finland. *Precamb. Research*, v. 21, p. 159~180.
- Park, B.K. (1972) Whole rock Rb-Sr age of the Seoul granite. *J. Geol. Soc. Korea*, v. 8, p. 156-162.
- Park, B.K. and So, C.S. (1973) The Ogcheon system in the central part of the southern Korea peninsula and global tectonics, *J. Geol. Soc. Korea*, v. 9, No. 3, p. 149-160 (in Korean).
- Park, B.K. and Do, I.K. (1974) The Mesozoic granitic batholiths in the Korean peninsula as an ancient island arc. *J. Geol. Soc. Korea*, v. 10, No. 4, p. 198-210 (in Korean).
- Pearce, J.A., Harris, N.B.W. and Tindle, A.G. (1984) Trace element Discrimination diagrams for the tectonic interpretation of granitic rocks. *J. Petrol.*, v. 25, p. 956-983.
- Powell, M. and Powell, R. (1977) Plagioclase-alkali feldspar geothermometry revisited. *Mineral Mag.*, v. 41, p. 253-256.
- Reedman, A.J. and Um, S.H. (1975) *The Geology of Korea*. Geol. Min. Inst. Korea, Seoul, 139pp.
- Saunders, A.D., Tarney, J. and Weaver, S.D. (1980) Transverse geochemical variations across the Antarctic peninsula: Implications for the genesis of calc-alkaline magma. *Earth Plan. Sci. Lett.*, v. 46, p. 344-360.
- Seo, K.S. (1985) Genesis of the Bupyeong Silver deposits. Unpubl. PhD thesis, Seoul Nat. Univ. 143pp (in Korean).
- Shaw, D.M., Dostal, J. and Keays, R. (1976) Additional estimates of continental surface Precambrian shields composition in Canada. *Geochim. Cosmochim. Acta.*, v. 40, p. 73-83.
- Sillitoe, R.H. (1975) Andean mineralisation: A model for the metallogeny of convergent plate margins. In: Strong, D.F. (ed), *Metallogeny and plate tectonics*. Geol. Assoc. Canada. Spec. paper, 14.
- Sillitoe, R.H. (1977) Metallogeny of an Andean-type Continental Margin in South Korea: Implications for opening of the Japan Sea. In: Talwani, M & Pitman, W.C. (eds), *Island-Arcs, Deep Sea trenches and Back-Arc Basins*. Maurice Ewing Series, I. Am. Geophys. Union, p. 303-310.
- Statham, P.J. (1976) A comparative study of techniques for quantitative analysis of the X-ray spectra obtained with a Si (Li) detector. *X-ray Spectrum*, v. 5, p. 16-28.
- Stormer, J.C. (Jr) (1975) A practical two-feldspar geothermometer. *Am. Mineral.*, v. 60, p. 667-674.
- Sun, C.O., Williams, R.J. and Sun, S.S. (1974) Distribution coefficients of Eu and Sr for plagioclase-liquid and clinopyroxene-liquid equilibria in oceanic ridge basalt: an experimental study. *Geochim. Cosmochim. Acta*, v. 38, p. 1415-1433.
- Sweatman, T.R. and Long, J.V.P. (1969) Quantitative electron-probe micro-analysis of rock forming minerals. *J. Petrol.*, v. 10, p. 332-379.
- Tarney, J. and Windley, B.F. (1977) Chemistry, thermal gradients and evolution of the lower continental crust. *J. Geol. Soc. London*, v. 134, p. 153-172.
- Tsuse, A., Mizuta, T., Watanabe, M. and Min, K.G. (1981) Jurassic and Cretaceous granitic rocks in South Korea. *Mining Geol.*, v. 31, No. 4, p. 261-280.
- Tsuse, A., Mizuta, T., Ohyoshi, A., Kim, S.W. (1984) Granitic rocks in the Gyeongsang basin, with particular reference to trace elements. In: *Granite provinces and associated ore deposits in South Korea—a comparison of granite and metallogenic pro-*

- vinces in South Korea and those in southwest Japan., Tsusue, A. (ed), 1-34.
- Ueda, N. (1969) Evolution of the continent in northeastern Asia, I: Reconnaissance survey of the geochronology of the Korean peninsula. J. Kor. Inst. Min. Geol., v. 2, No. 1, p.96-97.
- Uyeda, S. and Miyashiro, A. (1974) plate tectonics and the Japanese islands: A synthesis. Geol. Soc. Am. Bull. v. 85, p.1159-1170.
- Wood, D.A. (1979) A variably veined suboceanic upper mantle genetic significance for mid-Ocean ridge basalts from geochemical evidence. Geology, v. 7, p. 499-503.
- Workman, D.R. (1972) The tectonic setting of the Mesozoic granites in Korea. J. Geol. Soc. Korea, v. 8, No. 2, p.67-76.
- Yun, H.S. (1983) K/Ar ages of micas from Precambrian and Phanerozoic rocks in northeastern part of the Republic of Korea. Schweiz. Mineral. Petrogr. Mitt., v. 63, p.295-300.
- Yun, H.S. (1985) Petrochemical study on the granitic rocks in the southern Hambaeg Basin and its basement area. Unpubl. PhD thesis, Yonsei Univ., 147 pp. (in Korean).

韓國에 分布하는 先캄브리아紀, 쥬라紀 및 白堊紀花崗岩의 地化學的 特徵

洪 永 國

要約: 韓國에 分布하는 地質時代와 空間을 달리하는 代表的인 15個의 花崗岩體를 對象으로 鑛物 및 主·微量 元素 地化學的 特徵을 밝히고 岩石成因과 地體構造進化와 연관시켜 研究하였다. 그 岩石地化學的 特徵을 바탕으로 先캄브리아紀 花崗岩, 쥬라紀 花崗岩(cratonic과 mobile belt)와 白堊紀~第三紀 花崗岩으로 區分된다.

先캄브리아紀 花崗片麻岩(I-型 및 티탄鐵石系列)은 地化學的으로 進化된 花崗岩類가 變成作用을 받아서 形成 되었으며, 先캄브리아紀 花崗岩(S-型 및 티탄鐵石系列)은 堆積起源의 變成岩類가 部分熔融되어 生成된것으로 思 料된다.

쥬라紀 花崗岩(S-型 및 티탄 鐵石系列)은 주로 下部地殼의 變成堆積岩이 部分熔融되어 形成되었다. 또한, 白 堊紀花崗岩(I-型 및 磁鐵石系列)은 下部地殼 또는 上部맨틀의 火成源岩類로부터 生成된 마그마의 分別 結晶作用 으로 結晶化되었음이 밝혀졌다.

퍼다이트質 알카리長石의 溶離(exsolution)에 依한 地質溫度計는 先캄브리아紀 및 쥬라紀 花崗岩은 各 岩體內 그 溫度變化幅이 작으며($\pm 20 \sim 30^\circ\text{C}$), 約 3~5kbar의 假想壓力下에서 315~430°C의 낮은 溫度條件에서 化學的 平衡을 이룬것으로 나타났다. 이는 花崗岩貫入時 주위母岩들은 廣域變成作用과 같은 熱流量이 높은 영역下에 있 으며, 그 後 母岩은 花崗岩과 함께 천천히 冷却되었기 때문인 것으로 생각된다. 그러나, 白堊紀 花崗岩들은 各 岩體마다 1~3kbar 壓力下에서 520°C의 溫度에서 平衡을 이루었으며 그 變化幅($\pm 110^\circ\text{C}$)이 크다는 것으로 밝혀 졌는데, 이는 親마그마가 地表가까운 淺處까지 貫入하여 急速히 結晶化되었음을 示唆한다.

長石이 晶出될때의 酸素分壓은 沃川變成帶에 分布하는 쥬라紀 花崗岩이 가장 낮고, 慶尙盆地의 白堊紀 花崗岩 에서 높은 것으로 밝혀졌다.

쥬라紀 花崗岩(Hercyno-型)은 쿠라-퍼시픽(Kula-Pacific)板이 빠른 速度로 北西쪽으로 밀려와서 大陸間盆地 (Intracontinental basin)인 沃川盆地가 closing-collision으로 地殼下部의 部分熔融에 依하여 形成된 마그마(Wet magma)로부터 形成된 後 주위 母岩과 함께 隆起되었다. 白堊紀 花崗岩(Andino-型)은 쿠라-퍼시픽 海嶺의 Subduction에 依하여 生成된 마그마(Dry magma)가 構造的 弱線帶를 따라 빠른 速度로 地殼淺處까지 貫入되었다.